

# Higgs boson production under the resonance threshold at LEP II

E.Boos, M.Dubinin, L.Dudko

*Institute for Nuclear Physics, Moscow State University*

*119899 Moscow, Russia*

## Abstract

We consider the possibility of Higgs boson detection at LEP II under the resonance threshold ( $\sqrt{s} < m_H + m_Z$ ) in the framework of complete tree level approach to the calculation of the  $e^+e^- \rightarrow \nu\bar{\nu}b\bar{b}$  amplitude, simulating b-quark fragmentation to hadrons and taking into account typical detector properties. At the energy below the  $2m_Z$  threshold  $\sqrt{s} = 175$  GeV Higgs boson production under the  $m_H + m_Z$  threshold is almost background free.

## 1 Introduction

The possibility of Higgs boson detection in the four fermion final states at LEP II has been investigated recently on the level of complete tree level calculations, when the full set of diagrams (signal and irreducible background) is considered. In the papers [1, 2, 3] complete tree level calculation for the Higgs signal and irreducible backgrounds in the semileptonic four fermion processes

$$e^+e^- \rightarrow \mu^+\mu^-b\bar{b} \quad (1)$$

$$e^+e^- \rightarrow \nu\bar{\nu}b\bar{b} \quad (2)$$

$$e^+e^- \rightarrow e^+e^-b\bar{b} \quad (3)$$

has been done. In the processes (2) and (3) there are two types of signal diagrams for Higgs boson production (see Fig.1): 1) Higgs bremsstrahlung from the  $Z$ -boson line; 2) Higgs production by  $WW$  or  $ZZ$  fusion.

Higgs bremsstrahlung [4] and fusion [5] mechanisms taken separately (as the noninterfering amplitudes  $e^+e^- \rightarrow HZ$  and  $e^+e^- \rightarrow \nu_e\bar{\nu}_eH$ ) have been discussed for a long time. However it is much better to consider both mechanisms as the interfering parts of one amplitude (performing coherent summation of corresponding Feynman diagrams). The interplay of two mechanisms is especially interesting near the threshold energy  $\sqrt{s} = m_H + m_Z$  in the  $\nu_e\bar{\nu}_e b\bar{b}$  channel, when the contributions of Higgsstrahlung and fusion diagrams are of the same order and the interference term is positive and not negligible.

In particular it was shown [2] that in the process (2) at the energies  $\sqrt{s} < m_H + m_Z$  (under the threshold  $m_H + m_Z$ ) fusion mechanism is more important in the channel  $e^+e^- \rightarrow \nu_e\bar{\nu}_e b\bar{b}$  than Higgsstrahlung and can lead to observable events at LEP II luminosities. The number of events decreases as we go down in energy from the point  $\sqrt{s} = m_H + m_Z$  (or, equivalently, go up in Higgs mass from the point  $m_H = \sqrt{s} - m_Z$ ), but nevertheless in the mass interval of about 10 GeV under the threshold it could be possible to observe from four to ten Higgs production events/year. In other words, LEP II gives the possibility to look for the Higgs boson with the mass  $m_H = \sqrt{s} - m_Z + \Delta m$ , where  $\Delta m$  is about 10 GeV. Higgs peak could be observed in the invariant mass distribution of two b-jets and for this reason direct experimental reconstruction of two b-jets is very critical for signal separation [6].

The importance of fusion and interference terms in the threshold region has been mentioned in [6] and investigated in more details in [2] by means of Monte-Carlo simulation in the framework of complete tree level approach (23 diagrams in the  $\nu_e\bar{\nu}_e b\bar{b}$  channel, 11 diagrams in the  $\nu_\mu\bar{\nu}_\mu b\bar{b}$  and  $\nu_\tau\bar{\nu}_\tau b\bar{b}$  channels). Semianalytic results for the total cross section and analytic distributions for two signal diagrams and interference between them can be found in [7] where the 2  $\rightarrow$  3 body approximation  $e^+e^- \rightarrow \nu_e\bar{\nu}_eH$  has been used. Complete tree level semianalytic results for the 2  $\rightarrow$  4 body process (1) (25 diagrams) were obtained in [8]. However they are not extended yet to the case of fusion mechanisms.

The main purpose of present paper is the investigation of signal-background ratio in the process (2) under the threshold  $m_H + m_Z$  in the framework of complete tree level approach. The number of signal events is small at LEP

II luminosities and for this reason it is very important to have detailed understanding of the background taking into account some realistic properties of detector environment. For this reason we simulate b-quark fragmentation and employ some typical detector model for the calculation of  $M(b\bar{b})$  distribution.

Higgs production by  $ZZ$  fusion in the process (3) will also take place. However, the irreducible background diagrams give the cross section about 100 times larger than the signal and in this case we need nontrivial and complicated procedure of signal separation [3].

## 2 Cross sections

At present time several approaches exist (with the algorithmic realizations in the form of MC integrators or event generators) for the calculation of four fermion states at complete tree level. Description of general strategies can be found in [9]. We used CompHEP package [10] for complete tree level calculation of the signal and irreducible background. As usual, all possible squared diagrams and interferences between them (including signal-background interferences) were calculated. Fermion masses were kept nonzero in the amplitude calculation and four particle phase space generation. Two signal diagrams and 21 bias graphs for the process  $e^+e^- \rightarrow \nu_e\bar{\nu}_e b\bar{b}$  are shown in Fig.1. In the case of muon and tau neutrino in the final state the complete set of diagrams contains one signal and 10 bias graphs. All channels ( $\nu_e, \nu_\mu, \nu_\tau$ ) were taken into account in our simulation. Total cross sections of these processes at the energies  $\sqrt{s} = 175$  GeV and  $\sqrt{s} = 205$  GeV are shown in Table 1 for Higgs boson masses  $m_H = 85, 90, 95$  GeV and  $m_H = 115, 120, 125$  GeV respectively.

Two methods for the insertion of finite width in the  $H$  and  $Z, W$  propagators were used. The "fixed width" method implements the replacement

$$\frac{1}{k^2 - m^2 + i\epsilon} \rightarrow \frac{1}{k^2 - m^2 + im\Gamma}$$

in the resonant graphs only. Fixed width method violates the gauge invariance of the amplitude and at the same time does not affect nonresonant graphs. In the "overall" prescription the whole amplitude is multiplied by

the factor

$$\frac{k^2 - m^2 + i\epsilon}{k^2 - m^2 + im\Gamma}$$

preserving gauge invariance but obviously underestimating the contribution of nonresonant graphs. Besides this we would like to indicate one more drawback of the "overall" prescription. For instance, at the energy  $\sqrt{s} = 175$  GeV and Higgs boson mass  $m_H = 90$  GeV (see Table 1) the difference of results obtained by two methods is 25 %. In this case large contribution from the  $Z$  resonance is suppressed by the "overall" factor of Higgs propagator and vice versa. The case when  $Z$  and  $H$  peaks are close to each other gives one more example of the situation when the "overall" method cannot be applied for meaningful calculation. General discussion of the problem how to use boson propagators in the tree diagrams calculation at high energy can be found in [11]; although consistent results can be obtained in many cases by using different methods, the problem seems far from being understood completely.

The main background to Higgsstrahlung mechanism  $e^+e^- \rightarrow Z^*H^*$  is given by the processes  $e^+e^- \rightarrow Z^*Z^*$ ,  $e^+e^- \rightarrow Z^*\gamma^*$  (see second row of diagrams in Fig.1). Contrary to this situation the fusion mechanism  $e^+e^- \rightarrow \nu_e\bar{\nu}_eH$  under the  $2m_Z$  threshold is practically free from the background coming from  $e^+e^- \rightarrow \nu_e\bar{\nu}_eZ^*$  reaction (see third row of diagrams in Fig.1). This observation is especially important at the LEP II energy  $\sqrt{s} = 175$  GeV planned for the first stage of collider operation. For instance, at  $\sqrt{s} = 175$  GeV and  $m_H = 90$  GeV (5 GeV down the  $m_H + m_Z$  threshold) in the narrow width approximation we have for the signal

$$\sigma_{tot}(e^+e^- \rightarrow \nu_e\bar{\nu}_eH) * Br(H \rightarrow b\bar{b}) = 7.9 \text{ fb}$$

while a rough estimate for the resonant background (5 GeV down the  $2m_Z$  threshold)

$$\sigma_{tot}(e^+e^- \rightarrow \nu_e\bar{\nu}_eZ) * Br(Z \rightarrow b\bar{b}) = 0.79 \text{ fb}$$

In contrast to these numbers at  $\sqrt{s} = 205$  GeV the cross sections are 41.4 fb for the Higgs signal and 30.38 fb for the  $Z$  background. We performed more detailed calculations for the  $2 \rightarrow 3$  body background process  $e^+e^- \rightarrow \nu_e\bar{\nu}_eZ$  (9 Feynman diagrams). The contributions of two resonant graphs, the remaining 7 graphs as well as the negative interference between these two subsets are shown in Fig.2. If we go several GeV down the  $2m_Z$  threshold

the contribution of resonant graphs decreases approximately 10 times leaving the fusion mechanism of Higgs boson production practically background free. Signal and background cross sections are shown in Fig. 3.

Exact numbers (calculated using the  $2 \rightarrow 4$  body matrix element integrated over the four particle phase space) for the two signal mechanisms and interference between them as well as for the main (resonant) background graphs at the energies 175 GeV and 205 GeV are presented in Table 2. At the energy 205 GeV planned for LEP II upgrage (15 GeV above the  $2m_Z$  threshold) the contribution of main background graphs to the fusion mechanism increases about 10 times.

### 3 Simulation of the signal in the detector

We would like to consider in more details the practical possibility of signal detection at LEP II taking into account b-quark fragmentation and more or less realistic detector properties.

For this purpose we used the opportunity to switch on the external processes in the PYTHIA 5.7/JETSET 7.4 package [12]. For each event generated by CompHEP on the partonic level six four-momenta of initial and final particles and the total cross section were transferred to PYTHIA/JETSET as an input parameters. Fragmentation of b-jets, detector simulation and jet separation were done by means of JETSET. Independent fragmentation model (with the JETSET default parameters) was used. Detector simulation was performed by means of standard LUCCELL subroutine (contained in JETSET).

All space available for particle detection was divided into the cells of hadronic calorimeter. We used  $64 \times 80$  cells ( $\varphi_0 \times \eta$ ) with  $\eta = -\ln(\text{tg}(\vartheta/2))$  and  $-4 \leq \eta \leq 4$ . We introduced calorimeter resolution and the energy smearing in the detector cell. As usual the latter was defined corresponding to gaussian distribution with the standard deviation  $0.5 * \sqrt{E_{T \text{ cell}}}$  with the cutoff  $0 \leq E_{T \text{ smeared}} \leq 2 * E_{T \text{ true}}$  Detector granularity was chosen to be  $0.1 \times 0.1$ . The energy registered in the detector cell can be expressed as

$$(p_x, p_y, p_z, E, m)_{\text{cell}} = E_{T \text{ cell}} * (\cos\varphi, \sin\varphi, \sinh\eta, \cosh\eta, p^2/E_{T \text{ cell}})$$

At the next step we separated the jets from b-quarks. All detector cells with the energy greater than  $E_{T \text{ cell min}} > 5$  GeV were considered as jet initializer

cells. The energy of the cells near the initializer was summed if the distance in the  $\varphi, \eta$  parameter space  $\Delta R = \sqrt{\Delta\varphi^2 + \Delta\eta^2}$  was less than  $\Delta R = 0.5$  and considered as the hadronic cluster energy. If the cluster energy was greater than  $E_{T\ min} = 15$  GeV the cluster was identified as a jet.

We represent the invariant mass distributions of  $b\bar{b}$  at the partonic level and the jet-jet invariant mass distributions after fragmentation of b-quarks and detector simulation in Fig. 4-9. At the energy  $\sqrt{s} = 175$  GeV (Fig. 4-6) practically background free Higgs boson peak is observed if  $m_H + m_Z < 175$  GeV. Even in the case of Higgs and Z-boson peaks overlap  $m_H = m_Z$  which is the most complicated situation for the signal separation in Higgsstrahlung mechanism [13] the background is practically absent. At the energy  $\sqrt{s} = 205$  GeV (Fig. 7-9) the resonant background peak and the Higgs peak are observed.

## 4 Conclusion

Our analysis shows that the cross section of Higgs boson production under the threshold  $m_H + m_Z$  in the  $e^+e^- \rightarrow \nu\bar{\nu}b\bar{b}$  channel receives the very important contribution from the fusion mechanism additionally enhanced by the positive Higgsstrahlung-fusion interference. The cross section is rather small and the Higgs peak is strongly smeared by b-jet fragmentation process and the effects of limited detector resolution. Probably it would be hardly possible to reconstruct precisely the mass of Higgs resonance using the invariant mass distribution of two b-jets. However it seems realistic to observe some strong indication to the Higgs boson production at LEP II energies. The energy point  $\sqrt{s} = 175$  GeV is especially interesting for observation of the Higgs boson under the threshold. Detailed study of the background shows that at this energy (below the  $2m_Z$  threshold) the fusion mechanism of Higgs boson production is almost background free.

### Acknowledgements

The authors express their gratitude to the Centre of Theoretical Physics, Seoul National University where this work was completed. The research was partially supported by INTAS grant 93-1180.

## References

- [1] E.Boos, M.Sachwitz, H.J.Schreiber, S.Shichanin, Z.Phys. C61 (1994) 675  
G.Montagna, O.Nicrosini, F.Piccinini, Phys.Lett. B348 (1995) 496
- [2] M.Dubinin, V.Edneral, Y.Kurihara, Y.Shimizu, Phys.Lett. B329 (1994) 379  
E.Boos, M.Sachwitz, H.J.Schreiber, S.Shichanin, Int.J.Mod.Phys. A10 (1995) 2067
- [3] E.Boos, M.Sachwitz, H.J.Schreiber, S.Shichanin, Z.Phys. C64 (1994) 391
- [4] J.D.Bjorken, in: Proc.of Summer Institute on Particle Physics, ed.by M.Zipf, Stanford, 1976  
J.Ellis, M.K.Gaillard, D.V.Nanopoulos, Nucl.Phys. B106 (1976) 292  
B.L.Ioffe, V.A.Khoze, Phys.Elem.Part.At.Nucl.(USSR) 9 (1978) 118
- [5] D.R.T.Jones, S.T.Petcov, Phys.Lett. B84 (1979) 440  
G.Altarelli, B.Mele, F.Pitoli, Nucl.Phys., B287 (1987) 205
- [6] E.Boos, M.Dubinin, Phys.Lett. B308 (1993) 147
- [7] W.Kilian, M.Kramer, P.Zerwas, DESY preprint 95-216, 1995 (hep-ph/9512355)
- [8] D.Bardin, A.Leike, T.Riemann, Nucl.Phys. B, Proc.Suppl. 37B (1994) 274  
D.Bardin, A.Leike, T.Riemann, Phys.Lett. B344 (1995) 383  
D.Bardin, A.Leike, T.Riemann, Phys.Lett. B353 (1995) 513
- [9] F.A.Berends, R.Pittau, R.Kleiss, Nucl.Phys. B424 (1994) 308  
T.Ishikawa, T.Kaneko, K.Kato, S.Kawabata, Y.Shimizu, H.Tanaka, KEK report 92-19, 1993
- [10] E.Boos et al., Proc.of the XXVIth Recontre de Moriond, ed.by J.Tran Thanh Van, Editions Frontiers, 1991, p.501  
E.Boos et al., Proc.of the Int.Conf. on Computing in High Energy Physics, ed.by Y.Watase, F.Abe, Universal Academy Press, Tokyo, 1991, p.391  
E.Boos et al., SNU CTP preprint 94-116, Seoul, 1994 (hep-ph/9503280)

- [11] A.Aeppli, F.Cuyper, Geert van Oldenborgh, Phys.Lett., B314 (1993) 413  
E.Argyres, W.Beenakker, Geert van Oldenborgh, A.Denner, S.Dittmaier, J.Hoogland, R.Kleiss, C.Papadopoulos, G.Passarino, INLO-PUB-8/95 (hep-ph/9507216)
- [12] T.Sjostrand, M.Bengtsson, Comp.Phys.Comm., 43 (1987) 367  
H.-U. Bengtsson, T.Sjostrand, Comp.Phys.Comm., 46 (1987) 43
- [13] Z.Kunszt, W.Stirling, Phys.Lett., B242 (1990) 507  
N.Brown, Z.Phys., C49 (1991) 657



$\sqrt{s} = 175$ GeV									
$m_H, \text{GeV}$	85			90			95		
$\sigma_{tot}$ [fb] fixed $\Gamma$	34.8			20.0			16.0		
$\sigma_{tot}$ [fb] overall $\Gamma$	33.7			14.1			15.3		
channel	$\nu_e$	$\nu_\mu$	$\nu_\tau$	$\nu_e$	$\nu_\mu$	$\nu_\tau$	$\nu_e$	$\nu_\mu$	$\nu_\tau$
$\sigma_{tot}$ [fb] fixed $\Gamma$	17.9	8.4	8.4	11.2	4.4	4.4	8.7	3.6	3.6
$\sigma_{tot}$ [fb] overall $\Gamma$	17.3	8.2	8.2	6.9	3.6	3.6	8.2	3.6	3.6
$\sqrt{s} = 205$ GeV									
$m_H, \text{GeV}$	115			120			125		
$\sigma_{tot}$ [fb] fixed $\Gamma$	98.6			92.0			89.9		
$\sigma_{tot}$ [fb] overall $\Gamma$	98.2			91.6			89.6		
channel	$\nu_e$	$\nu_\mu$	$\nu_\tau$	$\nu_e$	$\nu_\mu$	$\nu_\tau$	$\nu_e$	$\nu_\mu$	$\nu_\tau$
$\sigma_{tot}$ [fb] fixed $\Gamma$	39.1	29.8	29.8	35.7	28.2	28.2	34.2	27.9	27.9
$\sigma_{tot}$ [fb] overall $\Gamma$	38.8	29.7	29.7	35.4	28.1	28.1	33.9	27.8	27.8

Table 1: Total cross sections for the the processes  $e^+e^- \rightarrow \nu\bar{\nu}b\bar{b}$ ,  $\nu = \nu_e, \nu_\mu, \nu_\tau$  calculated using two prescriptions for insertion of exact propagator in the amplitude. Parameter values  $m_b = 4.3$  GeV,  $m_Z = 91.19$  GeV,  $\Gamma_Z = 2.50$  GeV,  $\sin^2\vartheta_w = 0.225$ ,  $\alpha = 1/128$  were used.

$\sqrt{s} = 175 \text{ GeV}$			
$m_H, \text{GeV}$	85	90	95
Fusion mechanism	4.2	3.4	2.7
Higgsstrahlung mechanism	5.5	1.5	0.7
Interference	5.0	2.9	1.9
Total signal cross section	14.5	7.8	5.3
Background cross section	3.15		
$\sqrt{s} = 205 \text{ GeV}$			
$m_H, \text{GeV}$	115	120	125
Fusion mechanism	3.2	2.6	2.0
Higgsstrahlung mechanism	2.2	0.6	0.3
Interference	2.8	1.6	1.1
Total signal cross section	8.1	4.8	3.4
Background cross section	30.6		

Table 2: Signal and background cross sections (in  $fb$ ) for the  $2 \rightarrow 4$  process  $e^+e^- \rightarrow \nu_e \bar{\nu}_e b \bar{b}$ . The resonant background estimate given in section 2 (narrow width approximation) can be reproduced by  $2 \rightarrow 4$  calculation with the kinematical cut of 5 GeV around  $M(b\bar{b}) = m_Z$ .

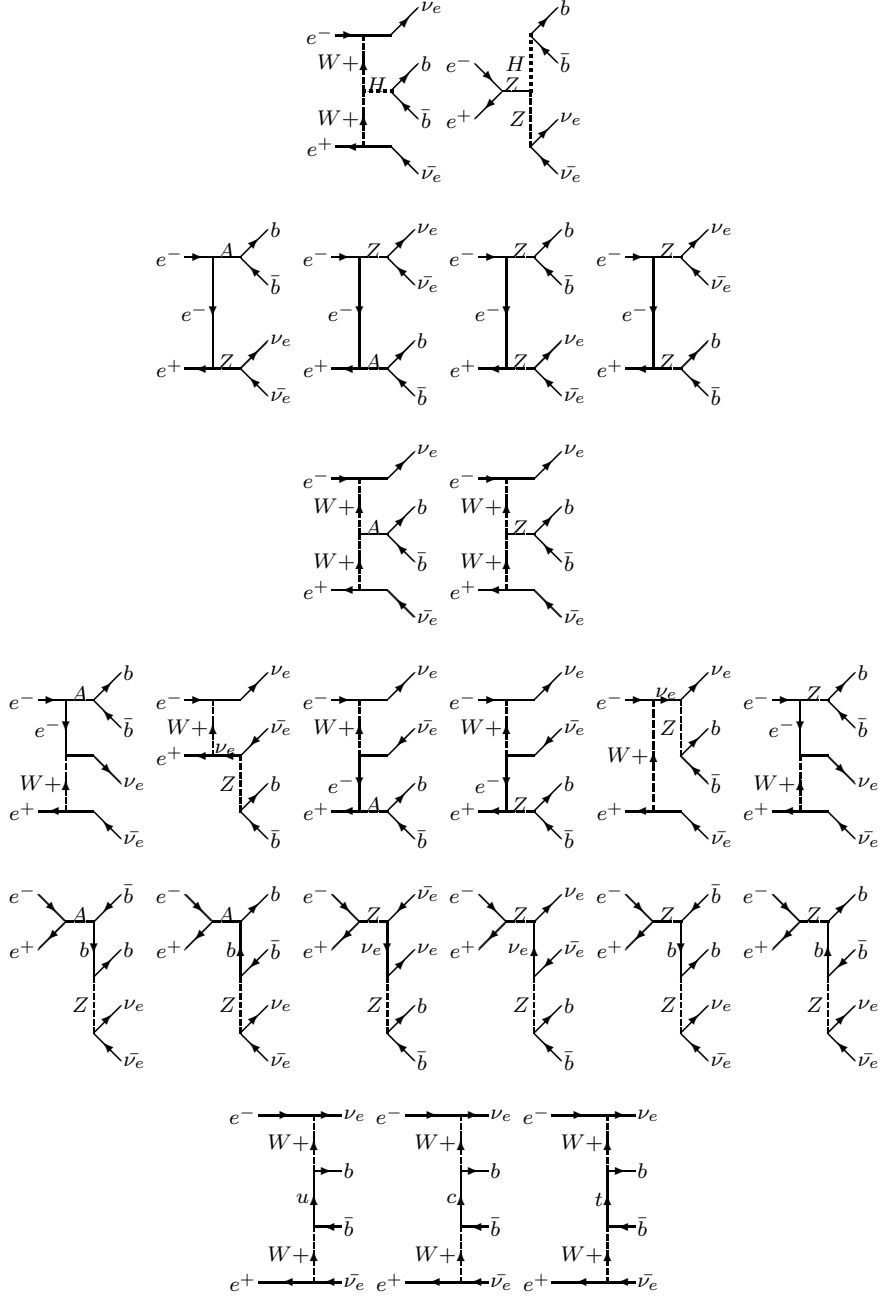


Figure 1: Complete set of diagrams for the process  $e^+e^- \rightarrow \nu_e \bar{\nu}_e b \bar{b}$

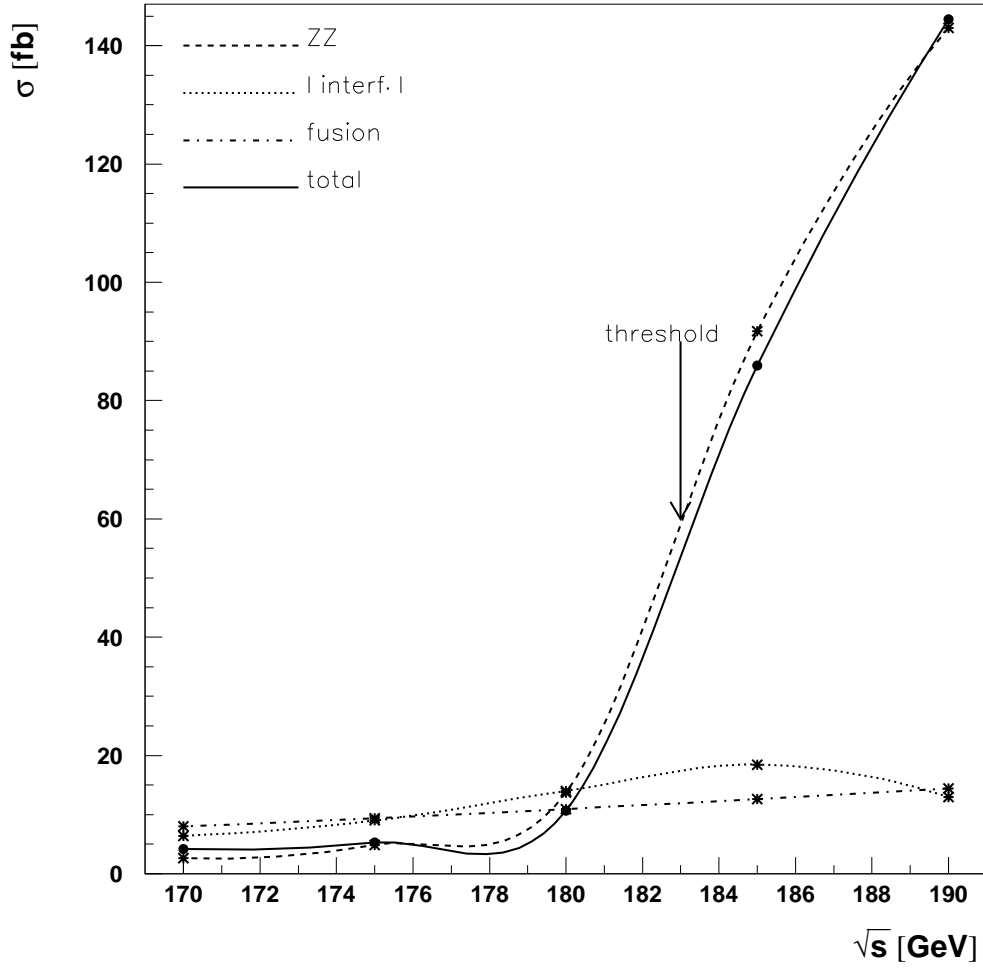


Figure 2: Total cross sections for the two subsets of diagrams (s-channel resonant diagrams as the first subset and all the rest as the second) and the interference between them in the process  $e^+e^- \rightarrow \nu_e\bar{\nu}_e Z$ . The absolute value of negative interference term is shown.

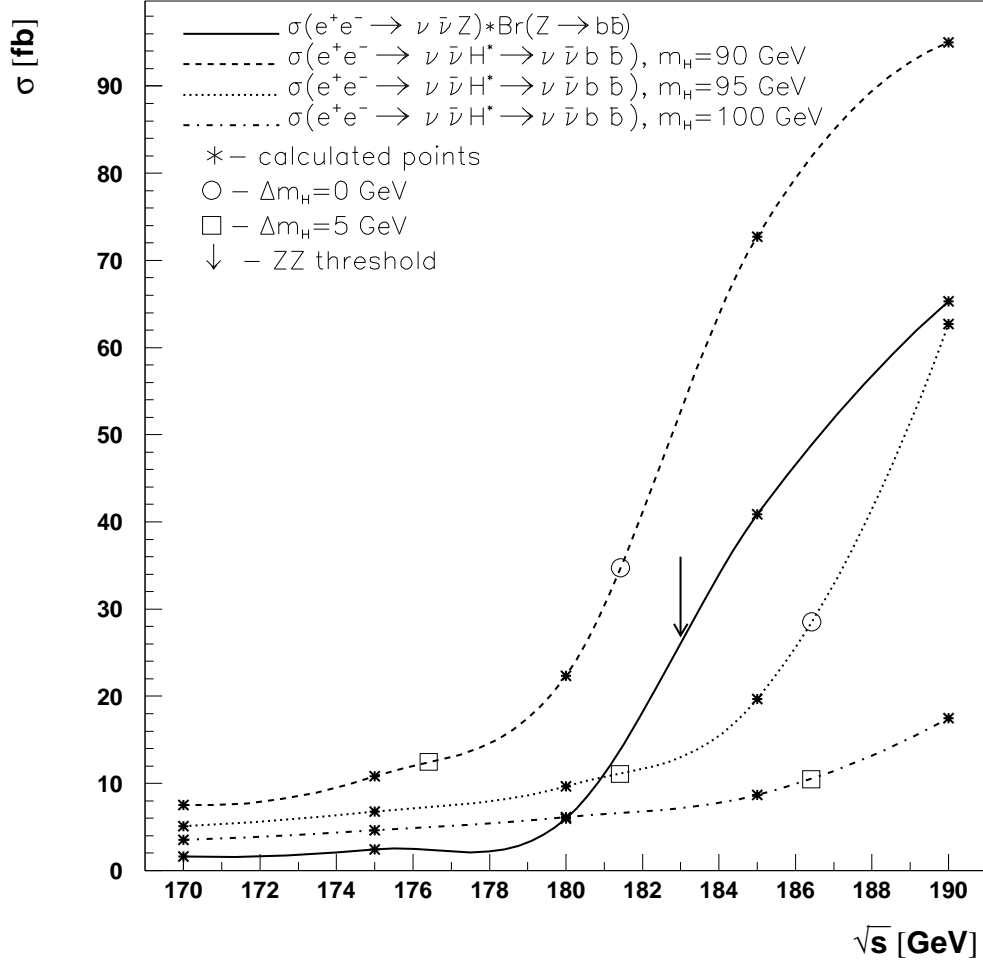


Figure 3: Background total cross section from Fig.2 together with the signal cross section  $e^+e^- \rightarrow \nu_e \bar{\nu}_e b \bar{b}$ . The distance from the  $HZ$  threshold  $\Delta m = -\sqrt{s} + m_H + m_Z$  in the cases  $m_H = 90, 95, 100$  GeV is marked on the corresponding cross section curves by the circles ( $\Delta m = 0$ ) and squares ( $\Delta m = 5$  GeV).

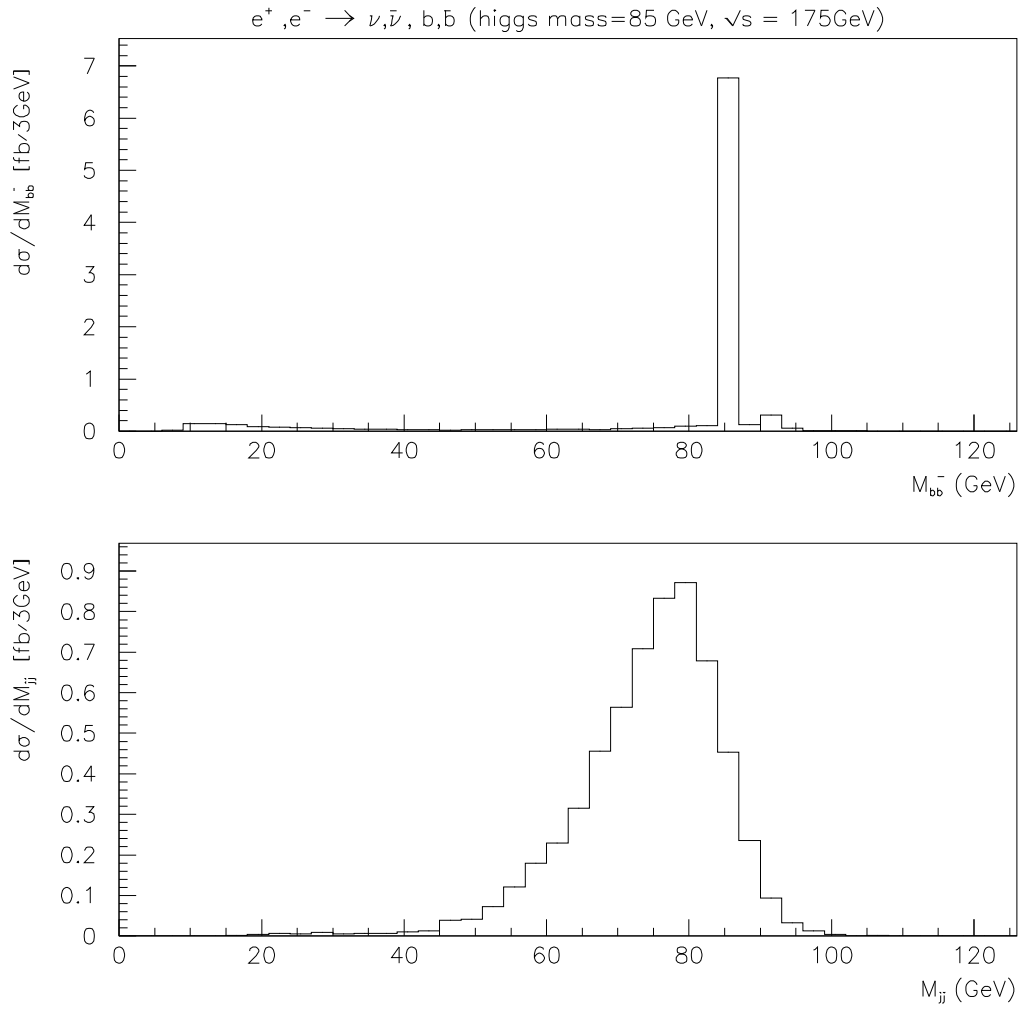


Figure 4:

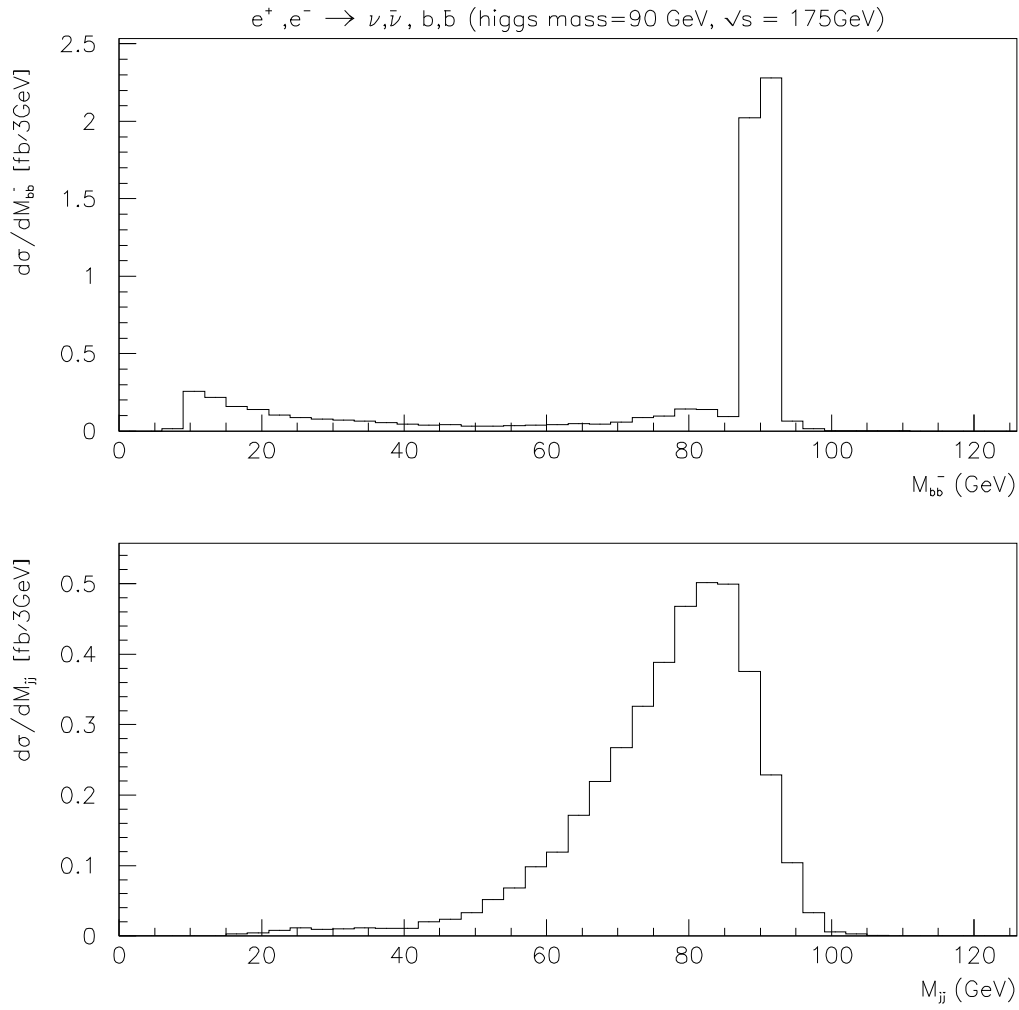


Figure 5:

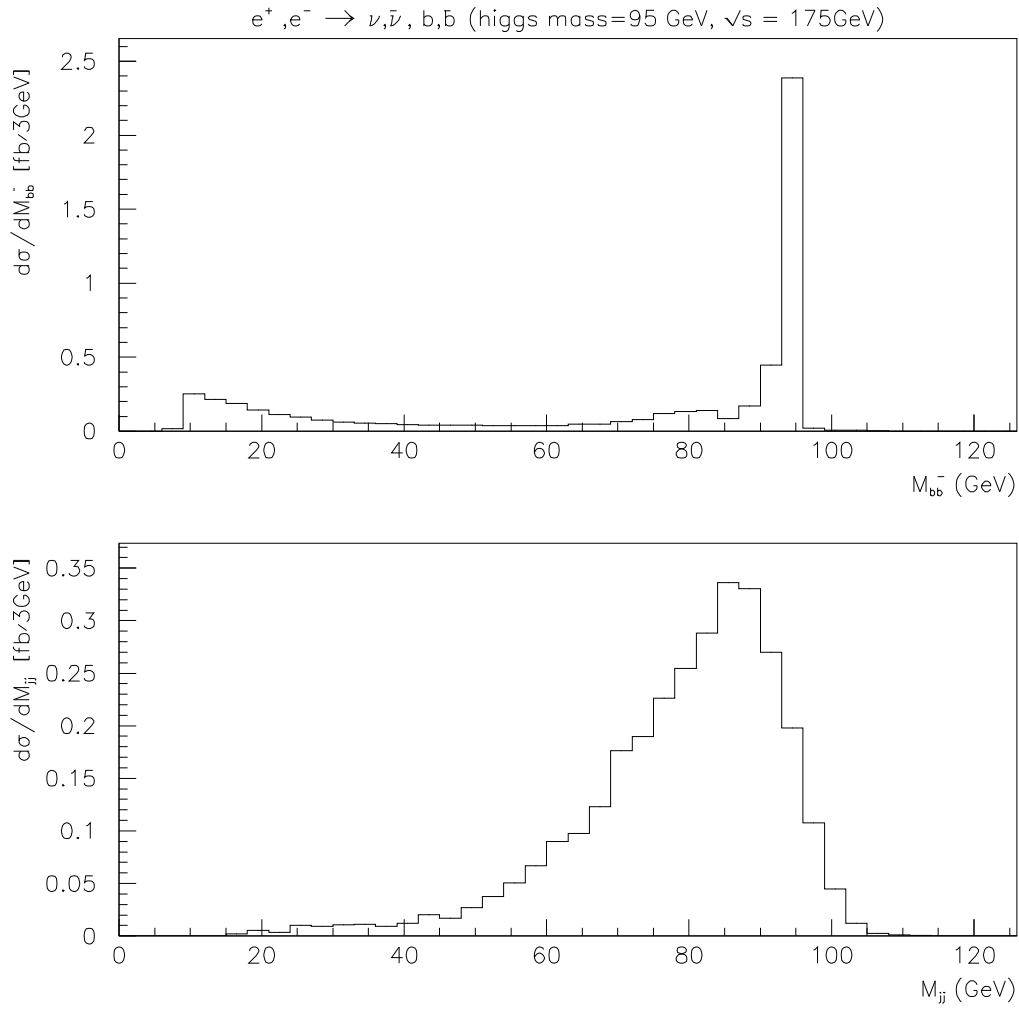


Figure 6:



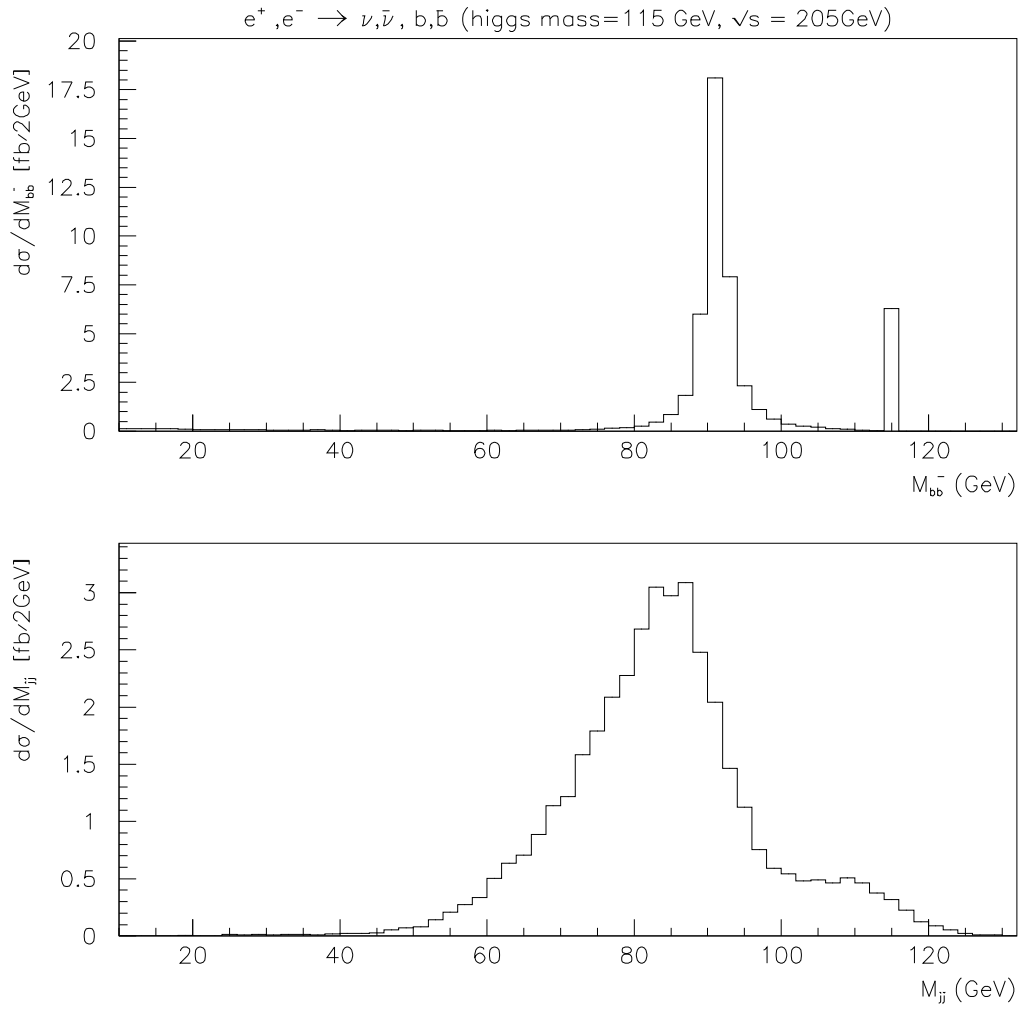


Figure 7:

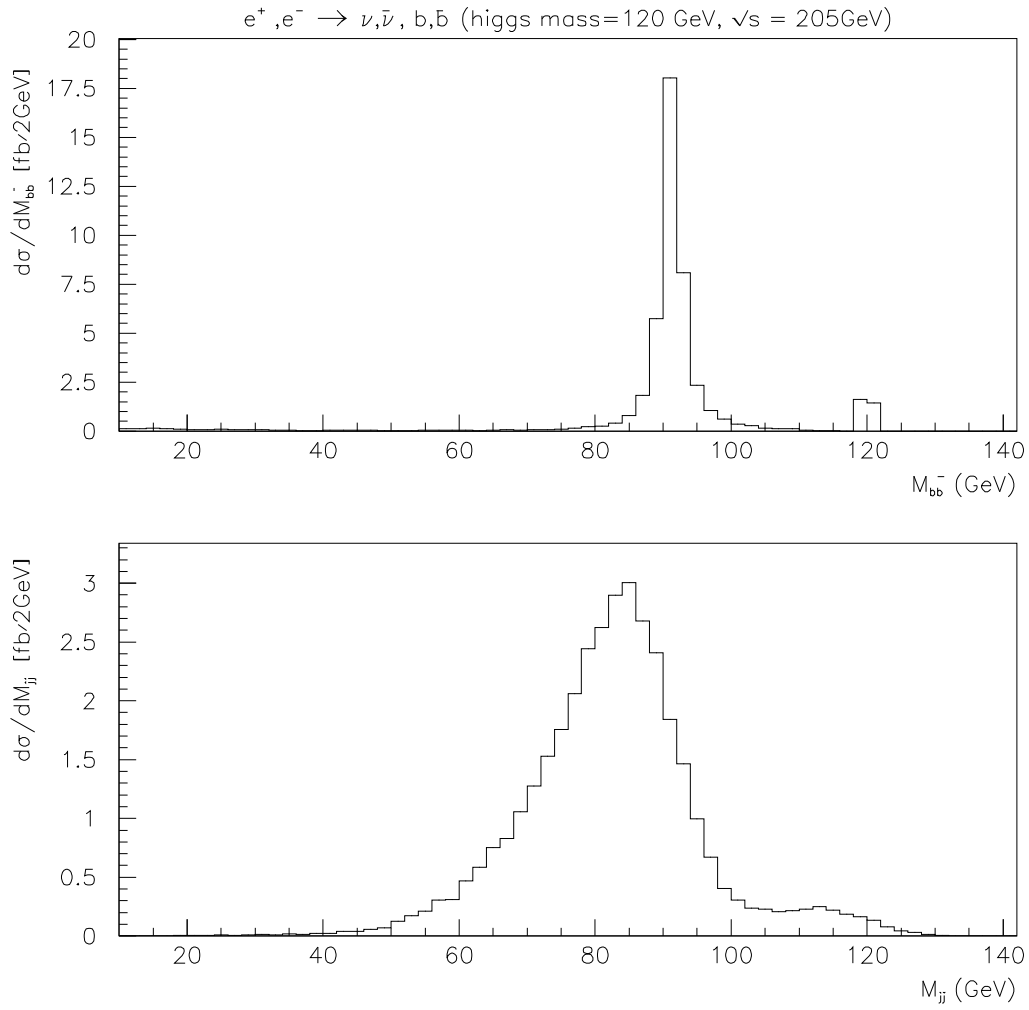


Figure 8:

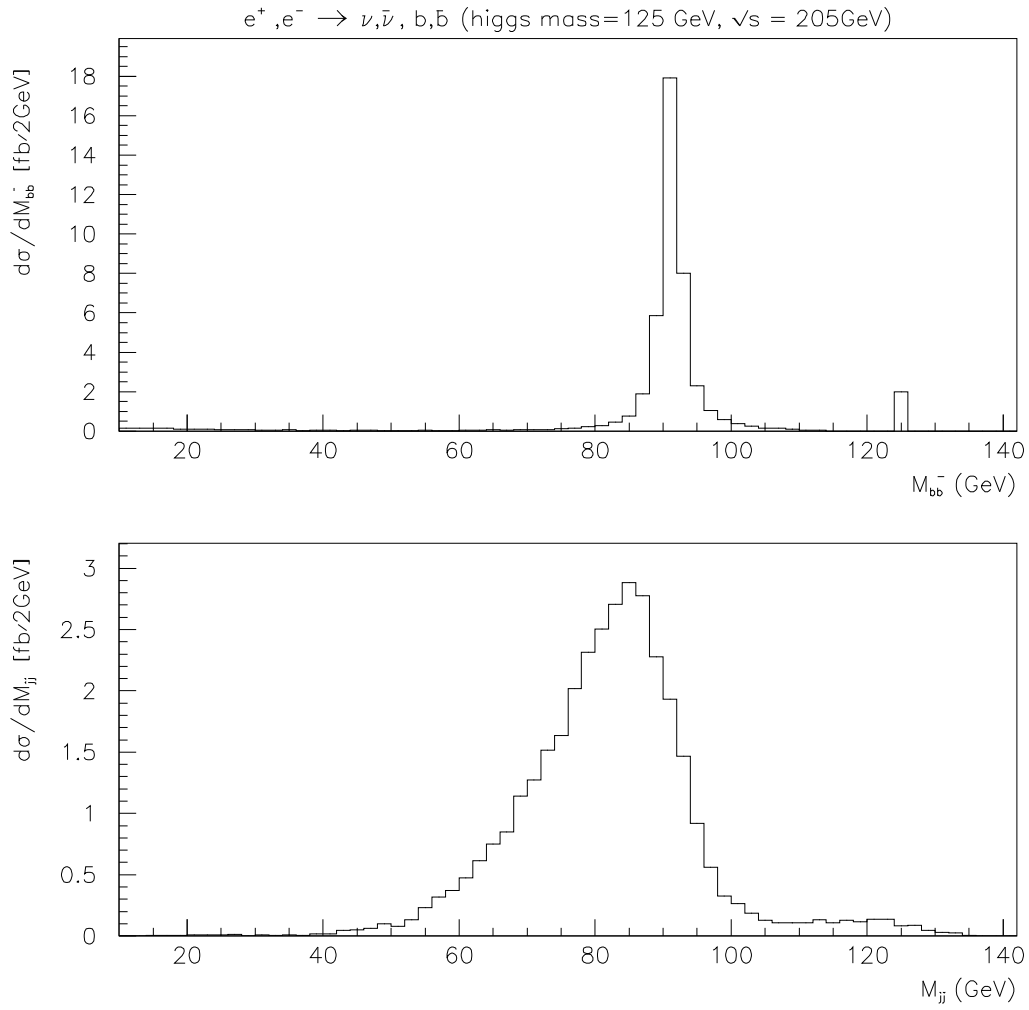


Figure 9: